

Lumped Circuit Ferrite Pulse Sharpener

M. Weiner

US Army Electronics Technology & Devices Laboratory, ERADCOM
Fort Monmouth, NJ 07703

S. Schneider

Southeastern Center for Electrical Engineering Education (SCEEE)
St. Cloud, FL 32769

F. Dollak

US Army Directorate for Management Information System (CECOM)
Fort Monmouth, NJ 07703

Summary

Ferrites are frequently employed as an auxiliary component in high voltage pulse circuits. The ferrite has a twofold purpose. One is to improve the pulse rise time in a low inductance circuit where the rise time is limited by the resistive fall time of the switch, typically a thyatron or an SCR. The other purpose is to reduce dissipation in the switch. The ferrite accomplishes these goals by behaving as a nonlinear inductor, or "saturable reactor". At about the same time that the switch becomes fully conducting, the ferrite inductance rapidly saturates, i.e., the pulse permeability quickly changes from a large value to a relatively small one.

In this paper the available design curves for the ferrite have been extended to include two additional effects: circuit inductance and the resistive fall time of the thyatron. Experimental results using magnesium manganese ferrite and an ITT F199 thyatron were obtained and compared with the complete model. The experimental results are in accord with the computer model.

Introduction

Ferrite materials have been used in high voltage pulse circuits for many years. The ferrite exhibits a saturation of the pulse permeability, which allows for the design of nonlinear inductors, or "saturable reactors". Such inductors, when used as an auxiliary element in a pulse circuit, are beneficial in two ways. First the pulse rise time is sharpened, and secondly, the dissipation in the main switch (typically a thyatron or SCR) is reduced. These desirable properties are achieved by virtue of the fact that, during the rise time portion of the pulse, when the main switch is undergoing ionization, the ferrite has a large effective inductance. During this time the bulk of the voltage is across the ferrite. The ferrite is designed so that when the main switch is fully ionized the ferrite permeability saturates, rapidly falling

from a large value to a relatively small one. At this point in time the voltage is transferred from the ferrite to the load, and since the ferrite is able to switch rapidly, the rise time of the pulse is sharpened. The switch dissipation is reduced by virtue of the fact that the ferrite inductor delays the passage of current during the commutation time.

There are two types of ferrite sharpeners. In the first the ferrite is distributed in a transmission line⁽¹⁾. In the second type, the ferrite is more concentrated and is considered a lumped circuit element. Generally the distributed type will offer a greater degree of sharpening, compared to the lumped ferrite. The lumped type, however, is notable for its simpler design and ease of interpretation. The theory for this type sharpener has been given previously⁽²⁾, and computer results were generated for the case of zero inductance. In this paper the computer model has been extended to include several additional effects. Computer results were obtained which take into account the circuit inductance as well as the commutation characteristics of a thyatron switch. Further, the transition of the ferrite from a nonlinear inductor to a linear one (after the ferrite saturates) is incorporated, thus strengthening the model. The extended model was compared with experimental results using magnesium manganese ferrite and a modified ITT F199 thyatron. In general the predictions of the model agree with the experimental observations.

Summary of Theory

The pulse circuit to be analyzed is shown symbolically in Fig. (1). The key element is the ferrite sharpener, which is assumed to be in the form of a toroid (or series of toroids) which surrounds the current carrying conductor of the pulse circuit. The nonlinear inductance of the ferrite arises from the motion of the magnetization under the influence of the magnetic field, produced by the pulse current. For a toroid the ferrite

Report Documentation Page				Form Approved OMB No. 0704-0188	
Public reporting burden for the collection of information is estimated to average 1 hour per response, including the time for reviewing instructions, searching existing data sources, gathering and maintaining the data needed, and completing and reviewing the collection of information. Send comments regarding this burden estimate or any other aspect of this collection of information, including suggestions for reducing this burden, to Washington Headquarters Services, Directorate for Information Operations and Reports, 1215 Jefferson Davis Highway, Suite 1204, Arlington VA 22202-4302. Respondents should be aware that notwithstanding any other provision of law, no person shall be subject to a penalty for failing to comply with a collection of information if it does not display a currently valid OMB control number.					
1. REPORT DATE JUN 1983		2. REPORT TYPE N/A		3. DATES COVERED -	
4. TITLE AND SUBTITLE Lumped Circuit Ferrite Pulse Sharpener of				5a. CONTRACT NUMBER	
				5b. GRANT NUMBER	
				5c. PROGRAM ELEMENT NUMBER	
6. AUTHOR(S)				5d. PROJECT NUMBER	
				5e. TASK NUMBER	
				5f. WORK UNIT NUMBER	
7. PERFORMING ORGANIZATION NAME(S) AND ADDRESS(ES) US Army Electronics Technology & Devices Laboratory, ERADOOM Fort Monmouth, NJ 07703				8. PERFORMING ORGANIZATION REPORT NUMBER	
9. SPONSORING/MONITORING AGENCY NAME(S) AND ADDRESS(ES)				10. SPONSOR/MONITOR'S ACRONYM(S)	
				11. SPONSOR/MONITOR'S REPORT NUMBER(S)	
12. DISTRIBUTION/AVAILABILITY STATEMENT Approved for public release, distribution unlimited					
13. SUPPLEMENTARY NOTES See also ADM002371. 2013 IEEE Pulsed Power Conference, Digest of Technical Papers 1976-2013, and Abstracts of the 2013 IEEE International Conference on Plasma Science. Held in San Francisco, CA on 16-21 June 2013. U.S. Government or Federal Purpose Rights License.					
14. ABSTRACT					
15. SUBJECT TERMS					
16. SECURITY CLASSIFICATION OF:			17. LIMITATION OF ABSTRACT SAR	18. NUMBER OF PAGES 5	19a. NAME OF RESPONSIBLE PERSON
a. REPORT unclassified	b. ABSTRACT unclassified	c. THIS PAGE unclassified			

magnetization satisfies (3)

$$\frac{d(M_z/M_0)}{dt} = \frac{2h}{S} (1 - M_z^2/M_0^2) \quad (1)$$

where

$4\pi M_z$ = Component of magnetization in direction of the field (gauss)
 $4\pi M_0$ = Saturation magnetization (gauss)
 h = Magnetic field (oersteds)
 S = Switching coefficient (oersted-sec)
 t = Time (sec)

From Eq. (1), one calculates the voltage induced in the ferrite, caused by the change in magnetic flux which occurs as the magnetization reverses direction. Initially the magnetization will be biased opposite to the direction of the pulse magnetic field. When the pulse is applied the reversal process is initiated, giving rise to the large effective inductance of the ferrite.

The ferrite is just one element in the pulse circuit shown in Fig. (1). The other elements are the main switch, the load (assumed to be a resistor for this analysis), the circuit inductance (including that in the main switch), and the pulse forming line. In this paper the main switch is assumed to be a thyatron, and during the commutation time, the thyatron possesses a source voltage V_t given by

$$V_t = V_0 (2 - e^{t/T_i}); 0 \leq t \leq T \quad (2)$$

where V_0 is the charge voltage, T_i is the effective ionization time of the tube, and $T = T_i \ln 2$. Beyond T the voltage across the thyatron is assumed to vanish, except for normal conduction loss and a possible inductive voltage drop. Another important time constant, aside from T , is $t = T_f$, the time at which the ferrite saturates, i.e., transitions from a nonlinear inductor to a linear type. In this model the transition is determined by matching solutions at T_f , assuming a constant, saturated permeability for the ferrite. T_f and T determine various intervals, with different solutions for each interval. For example, if $T_f < T$, the three intervals are $0 \leq t \leq T_f$, $T_f \leq t \leq T$, and $t \geq T$. Similar solutions are found when $T_f > T$.

Fig (2) shows typical theoretical waveforms of the load voltage and the voltage across the ferrite. Without ferrite the rise time is controlled by the resistive fall time of the thyatron, as modified by the circuit inductance. When ferrite is added the current is first delayed. When the ferrite saturates, at approximately 8 ns, the thyatron has already become fully conducting, and consequently the risetime is steeper. Obviously a steeper risetime will result only if the circuit is not overwhelmed by inductance. As noted in Fig (2), the ferrite voltage dominates during the commutation time of the switch.

Use of Computer Program

The input to the program consists of both the ferrite and circuit parameters (Table I). The pertinent equations are then solved and the voltage waveforms for the load resistance and ferrite plotted for the given set of parameters. The program also has the option of calculating an "optimum ferrite length", defined by $T_f = T$. Lengths which are longer often give steeper risetimes, however, and should be considered as well, provided the saturated ferrite inductance is not too large. The program also matches the voltage across the ferrite as it transitions from a nonlinear to a linear inductor. This procedure fixes the final M_z/M_0 value. In cases where the linear ferrite inductance is negligible the computer program may be simplified by specifying the final M_z/M_0 as an input. A value of 0.99 is usually sufficient.

Several important program inputs are not readily apparent or must be measured. One material property of the ferrite, the switching coefficient, is believed to be on the order of 0.10×10^{-6} oe-sec for large pulse fields. The saturated permeability is estimated from the slope of the hysteresis curve after saturation occurs at large fields. The initial ratio of M_z/M_0 is determined by the reverse bias. For sufficient reverse bias $M_z/M_0 \approx -1$.

Besides the ferrite properties the input circuit parameters must be estimated, particularly the circuit inductance and the resistive fall time of the thyatron. These two parameters may be obtained by auxiliary measurements. In the case of the fall time this means measurement of the tube or load voltage, while suppressing inductive effects by use of a large load resistance. In the case of the circuit inductance, the load waveform should be measured while using a small load resistance, in order to emphasize the inductive effects.

Experiment and Comparison with Theory

The experimental set-up was similar to that described previously⁽⁵⁾. Voltages across the F199 thyatron and the load resistance were measured with a Tektronix P-6015 or with other fast rise-time voltage probes. Current was measured with Tektronix CT-1. When measuring the ferrite voltage the ferrite was placed next to ground in the pulse circuit. No differences in the load waveforms were observed when the ferrite was above ground. Resistive fall time of the thyatron was controlled by variation of the reservoir voltage.

The dimensions of the magnesium manganese beads were: ID=0.25cm, OD=0.50cm, and length=1.25cm. No bias circuit was employed, but instead the load was negatively mismatched to a slight degree ($\approx 5\%$) so that the reverse pulse was used to bias the ferrite. The initial value of M_z/M_0 was assumed to be the ratio of the remanence (≈ 2000 gauss) to the saturation value

(≈ 3000 gauss), or -0.67 .

Preliminary comparisons of theoretical waveforms and the experiment are shown in Figs. (3)-(6). The ionization time of the thyatron was estimated from the tube voltage, ignoring inductive effects. No separate measurement for estimating the circuit inductance was made at this time. A circuit inductance of 0.2×10^{-6} h was assumed, plus a smaller ferrite inductance, after saturation. The ionization times (T_i) are approximately 15 ns and 28 ns for Figs (3) and (4) respectively. The load resistance was 50Ω . Because of experimental uncertainties in the zero time reference, the experimental and theoretical curves were arbitrarily matched at the points where the voltages were 25% of the final amplitude. In the experimental curves, the presence of current at $t=0$ indicates that the thyatron source voltage, eq. (2), should be modified to include a term describing the early stage of ionization in the tube. The observed current plateaus, which occur at about 75% of the maximum current, are believed to be caused by insufficient cathode emission. No such plateaus occurred when higher impedance loads (150Ω) were used. At the higher impedance levels, however, the degree of pulse sharpening observed was considerably lessened, in agreement with the theoretical predictions.

Fig (5) shows the comparison of the observed and theoretical ferrite voltage, taken at the higher reservoir setting. The agreement is reasonably good, given the complexity of the problem. Fig (6) compares the dissipation in the tube, with and without ferrite. The dissipation is obtained by obtaining the product of the voltage and current waveforms across the tube. The reduction in tube dissipation is evident in both the experimental and theoretical curves. The large dissipation observed near $t=0$, when no ferrite is used, is artificial. It relates to the aforementioned presence of current at $t=0$, and the need to modify the source voltage of the thyatron.

Conclusions

An improved computer model of the lumped circuit ferrite pulse sharpener has been developed. Comparison of the model and the experimental results indicates broad agreement. The initial design of the ferrite device may be accomplished using the present program. In order to make effective use of the program, however, the switch characteristics and the circuit inductance should be properly accounted for in the program, and this will require auxiliary measurements. The program itself is flexible in that adaptations of the program are routinely accomplished, such as changes in the switch characteristics or the use of a reactive load, instead of a resistive one.

The computer program also is adaptable to variations of the present ferrite device. For example, the sharpener may be improved by

interposing a long transmission line (transit time of line long compared to unsharpened rise time) between the switch and the remainder of the circuit. This has the effect of isolating the switch inductance, and its contribution to the risetime is rendered susceptible to being sharpened by the ferrite. Other types of sharpeners also may be described by the program.

1. M. Weiner, L. Silber, "Pulse Sharpening Effects in Ferrites" IEEE Trans. on Magnetics, Vol MAG-17, pp 1472-1477, July, 1981.
2. G. Mesyats, R. Baksht, "Deformation of Intense Waves Traversing a Ferrite Discontinuity in a Transmission Line", Soviet Physics - Technical Physics, Vol 10, pp 685-689, Nov, 1965.
3. E. Gyorgy, "Rotational Model of Flux Reversal in Square Loop Ferrites", J. Appl. Phys., Vol 28, pp. 1011-1015, Sept., 1957.
4. R. Caristi, S. Friedman, S. Merz, D. Turnquist, "New Developments in Super-Fast, High Power Hydrogen Thyatron Switching" IEEE Trans. Elect. Devices, Vol. ED-26, pp. 1927-1438, Oct. 1979.
5. S. Schneider, "Pulse Sharpening with a Series Ferrite Magnetic Switch In-Line-Type and Blumlein Modulators", Record of 15th Power Modulator Symposium, pp. 37-46, June 1982.

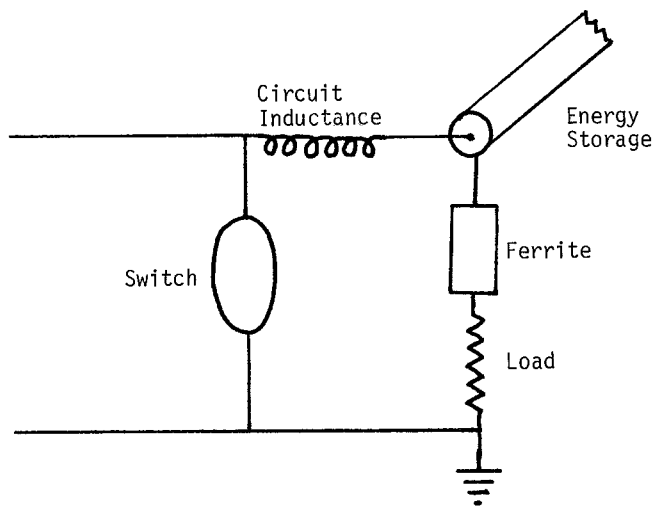


Figure 1: Ferrite Sharpener Circuit.

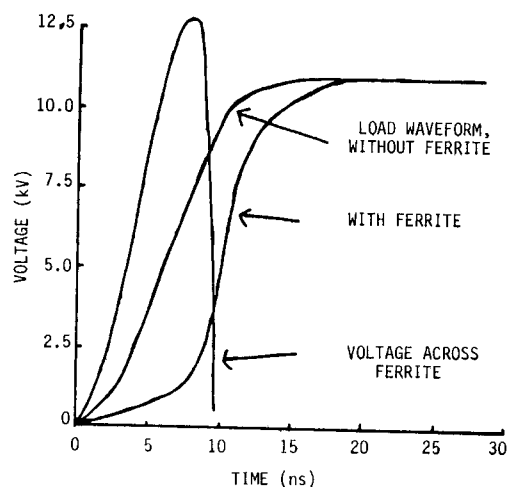


Figure 2: Computed voltage waveforms delivered to 50Ω load with and without ferrite. Also shown is ferrite voltage.

INPUT PARAMETERS OF FERRITE
PULSE SHARPENER PROGRAM

CIRCUIT	FERRITE
Initial Voltage	Inner Diameter of Ferrite
Circuit Inductance	Outer Diameter of Ferrite
Ionization Time of Tube	Total Length of Ferrite
Load Resistance	Saturation Magnetization
Characteristic Impedance of PFL	Saturated Permeability
	Switching Coefficient
	Initial M_z/M_0
	Final M_z/M_0

TABLE I

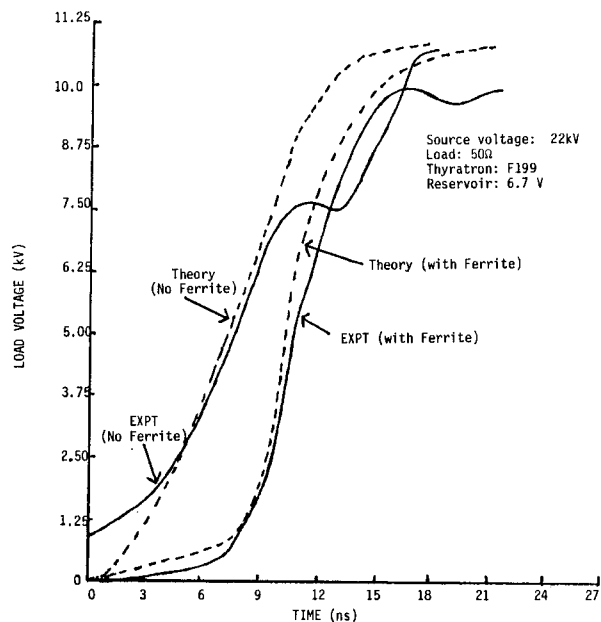


Figure 3: Comparison of theoretical and experimental load voltage waveforms. $T_i = 15$ ns.

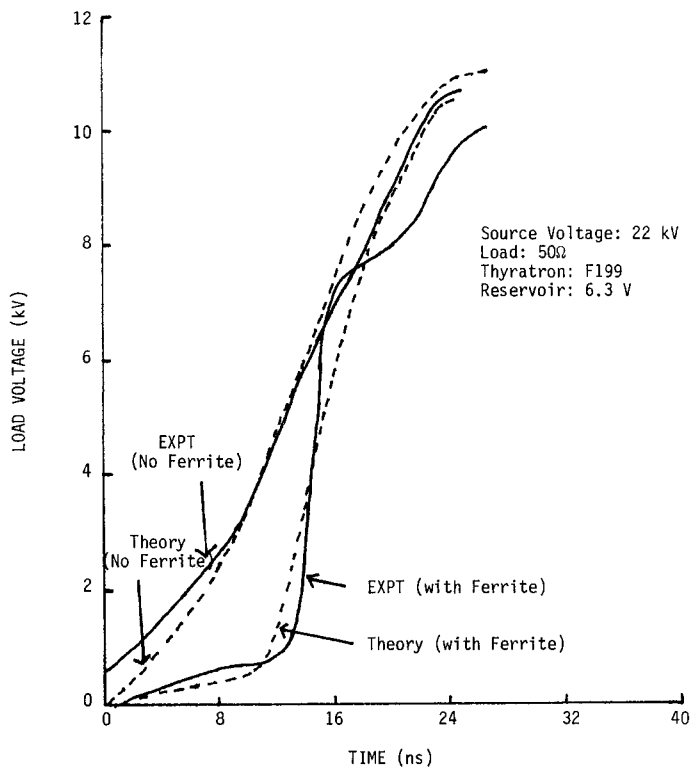


Figure 4: Comparison of theoretical and experimental load voltage waveforms. $T_i = 28$ ns.

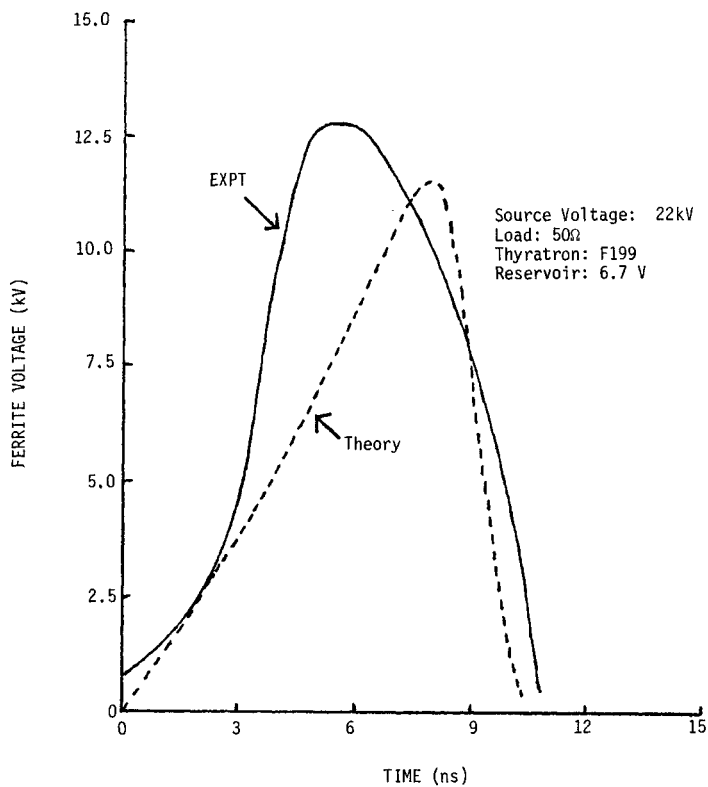


Figure 5: Comparison of theory and experiment for ferrite voltage.

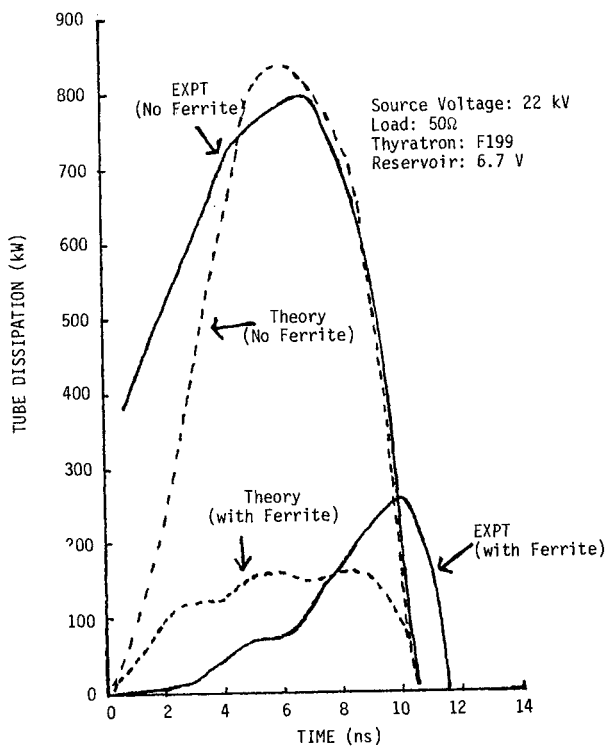


Figure 6: Comparison of theory and experiment for tube dissipation.